Separation Model for Two-Dimensional Airfoils in Transonic Flow

F.A. Dvorak* and D.H. Choi†
Analytical Methods, Inc., Redmond, Washington

A calculation method for transonic separated flow about two-dimensional airfoils at incidence has been developed. The method is capable of predicting the effects of both leading- and trailing-edge separated flows. A viscous potential flow iteration procedure provides the connection between potential flow, boundary layer, and wake modules. The separated wake is modeled in the potential flow analysis by thin sheets across which exists a jump in velocity potential. These sheets are analogous to vorticity sheets in incompressible flow. The agreement between theory and experiment for a series of airfoils is generally good even when shock waves are present.

Nomenclature

a = speed of sound
c = airfoil chord length
C_E = entrainment coefficient
C_f = skin friction coefficient
C_l = lift coefficient
C_p = static pressure coefficient
$H, \bar{H}$ = boundary-layer shape factors
M = Mach number
n = coordinate measured normal to the surface
q = $\sqrt{u^2 + v^2}$
r, θ = coordinates in σ plane
s = coordinate measured along the surface
T = temperature
U, V = velocity components in X and Y directions (incompressible flow)
u, v = velocity components in x and y directions (compressible flow)
X, Y = transformed coordinates, Eq. (9)
x, y = spatial coordinates in Cartesian or body-fitted system
z = physical plane
α = angle of incidence
γ = ratio of specific heats
δ = boundary-layer thickness
δ^* = boundary-layer displacement thickness
λ = $(\theta^2/\nu)(dU_e/dx)$
θ = boundary-layer momentum thickness
Λ = Polhausen parameter, $(\delta^2/\nu)(dU_e/dx)$
ν = fluid viscosity
ρ = fluid density
σ = computational plane
ϕ = velocity potential
ψ = stream function
ω = $(T_0 + 198.6)/(T + 198.6)\sqrt{T_w/T_0}$

Subscripts

e = evaluated at the edge of boundary layer
tr = transformed
0 = stagnation quantities
∞ = evaluated at the freestream state

Presented as Paper 83-0298 at the AIAA 21st Aerospace Sciences Meeting, Reno, Nev., Jan. 10-13, 1983; submitted Jan. 27, 1983; revision received Aug. 18, 1983.

*President, Director of Research. Associate Fellow AIAA.
†Research Scientist. Member AIAA.

Introduction

SEPARATED flow is one of the most important aspects of aerodynamics, as it is present in almost all applications of practical interest. However, separated flow, especially at transonic speeds, has received relatively little attention and a full analysis of this phenomenon has not yet achieved much success. It is, indeed, a challenging problem that requires not only a good inviscid transonic flow calculation method, but also an accurate prediction of boundary-layer development. Above all, in order to obtain efficiently any realistic solutions for which the large separated region exists, the wake region must be modeled appropriately.

Only a few investigators have attempted to model this complicated flow. Hicks[1] has coupled an optimization technique to an existing two-dimensional transonic airfoil code. He has been able to obtain separation profiles where the pressure remains constant along the separating streamline. Unfortunately, this procedure has not yet resulted in good agreement with experimental data. Diewert[2] has treated the two-dimensional airfoil with separation using a time-dependent Navier-Stokes code. Initial results for an 18% thick circular arc airfoil with a very small amount of trailing-edge separation are quite good; however, as the separated region increases, agreement with experiment deteriorates. Recently, Barnwell[3] proposed a calculation procedure for transonic flow with small amounts of trailing-edge separation. This method employs a closed-form solution of the boundary-layer equations in the reverse flow region. Limited comparisons with experiment show excellent agreement. Experience with a similar procedure developed by Cousteix[4] suggests that this approach can be successful for airfoils with small regions of separated flow, but must break down at large angles of attack where wake modeling becomes important.

The purpose of the present work is the development of an analysis method for predicting the performance of two-dimensional airfoils in transonic flow with the main emphasis placed on its modeling of the separated region. It is useful to note that a similar method for incompressible flow, CLMAX,[5] has been very successful in predicting the performance of two-dimensional airfoils having large regions of separated flow. The superior performance of CLMAX over other presently available methods has been confirmed by Blascovich's[6] recent study on evaluation of several representative separated flow airfoil analysis methods. In CLMAX, the wake surface is represented by a constant strength vortex sheet which, through iteration, assumes a force-free wake position. In the calculation method presented here, TRANMAX, the wake surface, is modeled by a discontinuity sheet with constant $\partial\phi/\partial s$ along it and with a jump in ϕ (tangential velocity) across it. This approach is analogous to the constant strength vorticity sheet model in CLMAX. The wake model in the present code is

closed and the shape remains fixed through one complete inviscid flow iteration cycle.

Jameson's code, FLO6,[7] with substantial change to include the wake region, is used for the inviscid flow calculation. The Cohen-Reshotko[8] boundary-layer method and Green's[9] turbulent lag-entrainment boundary-layer method are employed for the viscous flow calculations. The details of the procedure and its performance are described in subsequent sections.

Description of the Analysis Method

General Description

The present analysis method is built upon Jameson's two-dimensional potential flow calculation method, FLO6,[7] Cohen-Reshotko's laminar boundary-layer method,[8] and Green's lag-entrainment turbulent boundary-layer method.[9] These methods were verified thoroughly by their originators and can be used for transonic flow calculations with confidence.

The solution procedure is shown in Fig. 1. The initial potential flow solution is obtained either with or without the wake prescribed, depending on the initial separation point. The potential flow method has been substantially modified to model the separation region with the shape of the wake generated by a procedure to be described in a later section. The inviscid pressure distribution having been obtained, the boundary-layer development is predicted. This completes one viscid/inviscid calculation cycle.

In subsequent iterations, the induced normal velocity on the airfoil surface due to boundary-layer displacement effect is taken into account. A new wake is generated at the start of every iteration.

This procedure is repeated until the solution converges, i.e., the separation points between two successive iterations remain unchanged.

Details of individual elements are fully described in the following sections.

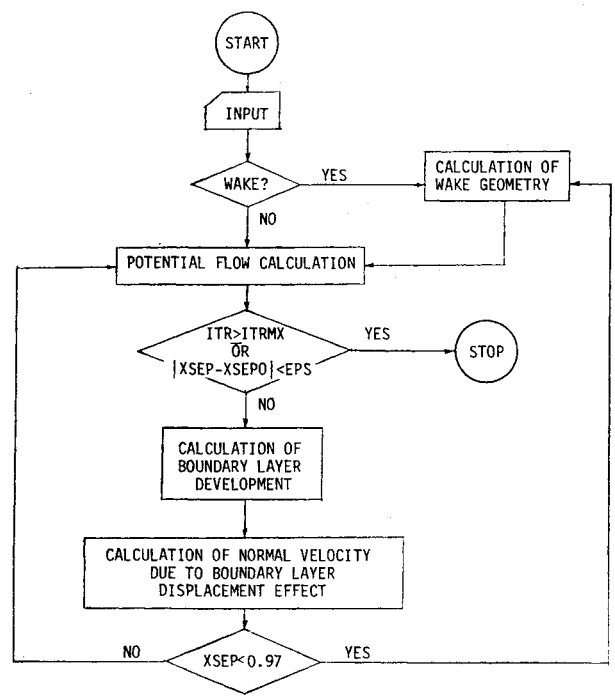

Fig. 1 Calculation procedure.

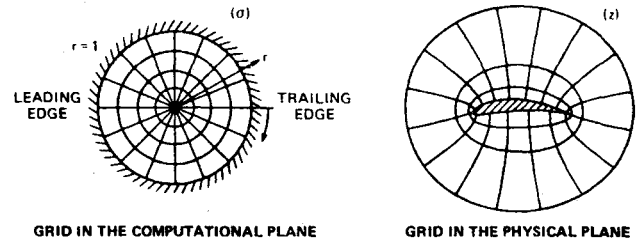

Fig. 2 Grid system.

Potential Flow Calculation Method

Basic Equations

From the equation of continuity and the momentum equation, we have

$$(a^2-u^2)\frac{\partial u}{\partial x}-uv\left(\frac{\partial u}{\partial y}+\frac{\partial v}{\partial x}\right)+(a^2-v^2)\frac{\partial v}{\partial y}=0 \quad (1)$$

Assuming irrotational flow, a velocity potential, ϕ, can be defined, i.e.,

$$u=\frac{\partial \phi}{\partial x}, \qquad v=\frac{\partial \phi}{\partial y} \quad (2)$$

Substitute these into Eq. (1) to obtain

$$(a^2-u^2)\phi_{xx}-2uv\phi_{xy}+(a^2-v^2)\phi_{yy}=0 \quad (3)$$

This equation can be solved for ϕ with the use of the energy equation

$$a^2+\frac{\gamma-1}{2}q^2=\left(\frac{1}{M_\infty^2}+\frac{\gamma-1}{2}\right)q_\infty^2 \quad (4)$$

where $q=\sqrt{u^2+v^2}$. The Neumann boundary condition is prescribed along the surface: $\partial\phi/\partial n=0$ is set initially, and it takes a new value which reflects the viscous effect after each iteration cycle.

$$\frac{\partial \phi}{\partial n}=0 \qquad \text{(first iteration)}$$

$$=\frac{1}{\rho}\frac{\partial}{\partial s}(\rho u\delta^*)=f \qquad \text{(subsequent iterations)} \quad (5)$$

where δ^* is the boundary-layer displacement thickness and s is measured along the airfoil surface.

Because the nature of Eq. (3) is hyperbolic if the local Mach number $M=q/a>1$ and elliptic if $M<1$, it is essential to transform the infinite flowfield onto a finite domain. This can be achieved by mapping the exterior of the airfoil in the z plane conformally onto the interior of a unit circle in the σ plane as shown in Fig. 2, taken from Ref. 10.

This transformation is particularly useful because an evenly distributed grid system in the circle plane gives denser finite mesh near the body at the leading and trailing edges in the physical plane where it is needed most.

Inviscid Model of Separated Region

As mentioned earlier, the modeling of the wake is one of the more important elements in the method. One may solve the parabolized Navier-Stokes equations for the special class of flow instead of modeling the wake. However, in principle this cannot handle the region of large reverse flow. On the other hand, solving the full time-dependent Navier-Stokes equations is not practical at this time because of the enormous computing time required. The only logical approach to this problem is to simulate the separated flow with an inviscid wake model. A good wake model, in fact, can represent the actual flow very well as was demonstrated by an earlier study (CLMAX).[5]

In the present model, the separated region is confined by two dividing streamlines, one from the upper surface separation point and the other from the trailing-edge point, as shown in Fig. 3.

As shown in the figure, along the dividing streamlines the gradient in velocity potential, $\partial\phi/\partial s$, is constant, while across the streamlines, $\partial\phi/\partial n$ is zero.

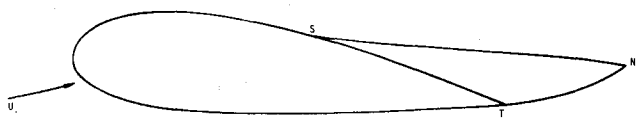

Fig. 3 Wake model.

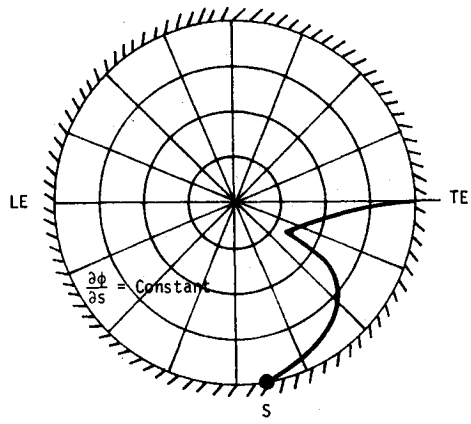

Fig. 4 Separated region in the computational plane.

The wake shape is updated for each new calculated separation point. If the separation point remains unchanged, then the solution is considered to be converged.

Construction and Transformation of the Wake

The wake model employed in this study has the form of two parabolas, one from the upper surface separation point and the other from the trailing edge (see Fig. 3). The initial slopes of these parabolas assume the surface tangents at their respective points. These two curves are joined together at some point downstream of the trailing edge (usually 20-30% of the chord length) which is in line with the earlier model in CLMAX.

This wake in the physical plane can now be transformed onto the circle plane. First, the grid network on the physical plane, which corresponds to the uniform grid in the circle plane, is generated by using the mapping function. With the aid of simple interpolation, the wake in the physical plane can be readily transformed onto the circle plane. A typical resulting separated region in the circle plane is shown in Fig. 4.

The streamlines which divide the flow into attached and separated flow regions represent lines of constant $\partial\phi/\partial s$. These streamlines represent thin shear layers across which there exists a jump in tangential velocity; and, consequently, a jump in velocity potential, ϕ. Due to this jump a special treatment in the finite difference procedure is necessary along this boundary. In the present method, the value of ϕ is adjusted up or down by the amount of jump, $\Delta\phi$, where

$$\Delta\phi_i = \frac{\partial\phi}{\partial s}\Delta s_i$$

and Δs is measured from point S or T, depending on the particular side, to make the function ϕ continuous across the dividing streamline. With this addition and subtraction, the same difference formulas can be used throughout the field. The procedure is similar to the so-called "shock fitting" technique.

The Kutta condition, which is normally applied at the trailing edge, is applied at points S and T, i.e.,

$$\left.\frac{\partial\phi}{\partial s}\right|_S = \left.\frac{\partial\phi}{\partial s}\right|_T \tag{6}$$

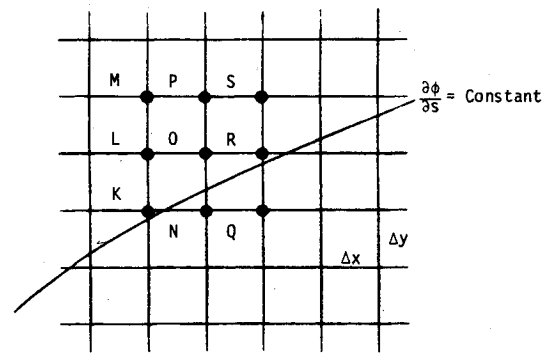

Fig. 5 Finite difference grid.

Special Treatment in Finite Difference Formulas along the Dividing Streamline

The main idea of present finite difference formulas near the dividing streamline is to make the potential, ϕ, continuous across this streamline. As previously mentioned, this can be achieved by adding or subtracting the amount of jump, $\Delta\phi$, to or from ϕ at a particular point. The correction is applied to all points lying on the side opposite the point of finite difference approximation.

For example, the derivatives about the point 0 are shown below (see Fig. 5)..

$$\frac{\partial\phi}{\partial x} = \frac{\phi_R - \phi_L}{2\Delta x} \tag{7a}$$

$$\frac{\partial\phi}{\partial y} = \frac{\phi_P - (\phi_N + \Delta\phi_N)}{2\Delta y} \tag{7b}$$

where

$$\Delta\phi_N = \left.\frac{\partial\phi}{\partial s}\right|_{\text{at separation}} \Delta s_N$$

Δs_N = arc length along the dividing streamline

$$\frac{\partial^2\phi}{\partial x^2} = \frac{\phi_R - 2\phi_0 + \phi_L}{\Delta x^2} \tag{7c}$$

$$\frac{\partial^2\phi}{\partial y^2} = \frac{\phi_P - 2\phi_0 + (\phi_N + \Delta\phi_N)}{\Delta y^2} \tag{7d}$$

$$\frac{\partial^2\phi}{\partial x\,\partial y} = \frac{\phi_S - \phi_M + \phi_K - (\phi_Q + \Delta\phi_Q)}{4(\Delta x\Delta y)} \tag{7e}$$

Method of Solution

The governing Eq. (3), together with the boundary condition, Eq. (5), is solved by a finite difference scheme after being transformed onto a unit circle. Upwind differencing is used when the local flow is supersonic, while central difference formulas are used at subsonic points. The resulting set of difference equations is solved iteratively. Details of the method are referred to in the original paper[7] and only the major differences are presented here.

The Kutta condition is imposed by matching the pressures at the upper surface separation point and the trailing edge, i.e.,

$$\left.\frac{\partial\phi}{\partial s}\right|_{\text{sep}} = \left.\frac{\partial\phi}{\partial s}\right|_{\text{trailing edge}} \tag{6'}$$

The amount of circulation is continuously updated to satisfy Eq. (6). The new estimate of circulation determined from the Kutta condition is then used for the next iteration. This cycle is repeated until the correction to the old circulation value satisfies the convergence criteria.

It was found during the course of this work that the method may encounter some difficulty if the solution is sought directly for freestream Mach numbers greater than 0.35. This occurs because the actual flow is becoming less stable and will respond rapidly to even small disturbances. When the separation region is large (greater than 10% chord), the initial inviscid flowfield is not representative of the flowfield with separation; consequently, a poor initial solution can lead to divergent behavior at higher Mach numbers. Proper convergence and stability can be achieved by starting the solution from a low Mach number and raising the Mach number incrementally to the desired value.

After the velocity potential, ϕ, is obtained, the tangential velocity component, u, on the surface can be obtained readily through simple differencing. The pressure coefficient C_p along the surface is given by

$$C_p = \frac{1}{(\gamma/2)M_\infty^2}\left\{\left[1+\frac{\gamma-1}{2}M_\infty^2(1-u^2)\right]^{\gamma/\gamma-1}-1\right\} \quad (8)$$

Calculation of Boundary-Layer Development

The boundary-layer development along both upper and lower surfaces is calculated by Cohen-Reshotko's laminar boundary-layer method[8] and Green's turbulent boundary-layer method.[9] The Granville procedure is adopted as a transition criterion[11] and the possibility of the reattachment as a turbulent boundary layer after laminar boundary-layer separation is also examined on the basis of the Reynolds number based on the momentum thickness at the point of separation.[11]

Cohen and Reshotko Method

This integral method was developed for the steady two-dimensional laminar boundary layer with the assumption that the surface temperature is uniform. First, consider the Stewartson transformation

$$\frac{\partial\psi}{\partial y}=\frac{\rho u}{\rho_0} \qquad \frac{\partial\psi}{\partial x}=\frac{-\rho v}{\rho_0}$$

$$X=\int_0^x \omega\frac{a_e}{a_0}\frac{p_e}{p_0}\,dx \qquad Y=\frac{a_e}{a_0}\int_0^y\frac{\rho}{\rho_0}\,dy$$

$$U=\frac{\partial\psi}{\partial y} \qquad V=-\frac{\partial\psi}{\partial x} \quad (9)$$

where ψ and a represent the stream function and the speed of sound, respectively. Capital letters denote quantities of the equivalent incompressible problem. With this transformation, the equivalent incompressible problem can be formulated.

The momentum integral equation in two-dimensional flow is given by

$$\frac{d\theta_{tr}}{dX}+\frac{\theta_{tr}}{U_e}\frac{dU_e}{dX}(H_{tr}+2)=\frac{C_f}{2} \quad (10)$$

where C_f is the skin friction coefficient $\tau_w/\frac{1}{2}\rho U_e^2$, and the subscript tr denotes the transformed (incompressible) coordinate. Introducing a parameter λ where

$$\lambda=-\frac{\theta_{tr}^2}{\nu_0}\frac{dU_e}{dX} \quad (11)$$

and substituting this into Eq. (10) gives

$$-U_e\frac{d}{dX}\left[\frac{\lambda}{(dU_e/dX)}\right]=2\left[\lambda(H_{tr}+2)+\frac{C_f}{2}\right] \quad (12)$$

The right-hand side of this equation can be approximated by a linear function of λ,[8,12] i.e., $C_1+C_2\lambda$, and, therefore, the ordinary differential equation (12) has an analytical solution,

$$\lambda=-C_1U_e^{-C_2}\frac{dU_e}{dX}\int_0^X U_e^{C_2-1}\,dX \quad (13)$$

where the arbitrary constant vanishes to ensure a finite momentum thickness at the stagnation point. The Stewartson transformation finally leads us to

$$\lambda=-C_1M_e^{-C_2}\frac{dM_e}{dx}T_e^{-4}\int_0^x M_e^{C_2-1}T_e^4\,dx \quad (14)$$

This can be readily solved for λ by simple integration formulas such as the trapezoidal rule. Then the momentum thickness and the shape factor H are obtained from the explicit expressions of λ.

The separation of the boundary layer is detected by examining the Polhausen parameter, $\Lambda=\delta^2/\nu(dU_e/dx)$, assuming that the H-Λ table for the incompressible flow is still valid.

After transition, either through natural transition or through a separation/reattachment process, Green's method takes over the calculation of downstream turbulent boundary-layer development.

Green's Method

This is a "lag-entrainment" integral method involving three equations: momentum-integral, entrainment equation, and a rate equation for the entrainment coefficient.[9] The method is a combination of Head's original entrainment momentum-integral method and the turbulent model proposed by Bradshaw et al. in which the algebraic relation for the entrainment coefficient of Head's method is replaced by a rate equation derived from the turbulent kinetic energy equation.

The resulting equations are:

$$\frac{d\theta}{dx}=F_1(\theta,\overline{H},C_E) \quad (15)$$

$$\frac{d\overline{H}}{dX}=F_2(\theta,\overline{H},C_E) \quad (16)$$

$$\frac{dC_E}{dx}=F_3(\theta,\overline{H},C_E) \quad (17)$$

where

$$\theta=\int_0^\infty\frac{\rho u}{\rho_e u_e}\left(1-\frac{u}{u_e}\right)dy, \qquad \overline{H}=\frac{1}{\theta}\int_0^\infty\frac{\rho}{\rho_e}\left(1-\frac{u}{u_e}\right)dy$$

$$C_E=\frac{1}{\rho_e u_e}\frac{d}{dx}\int_0^\delta\rho u\,dy$$

This system of ordinary differential equations is solved by the Runge-Kutta method. The separation point can be located by monitoring both the friction coefficient C_f and the shape factor H.

Results and Discussion

The main purpose of this analysis method is the prediction of the performance of a given airfoil for a wide range of angles of attack from which the maximum lift and its corresponding angle can be determined. As will be shown in this section, the analysis performs very well for all the cases examined. Pressure distributions, as well as lift and moment curves, are in good agreement with experimental data.

The method has been tested against three distinctly different airfoils: the GA(W)-1,[13] the NACA 0012,[14] and the Model A1.[15] The freestream Mach number varies from 0.15 for the GA(W)-1 to 0.6 for the A1 airfoil. For each flow condition the angle of attack is gradually increased until the airfoil has stalled. Airfoils at angles of attack beyond the static stall angle have been analyzed.

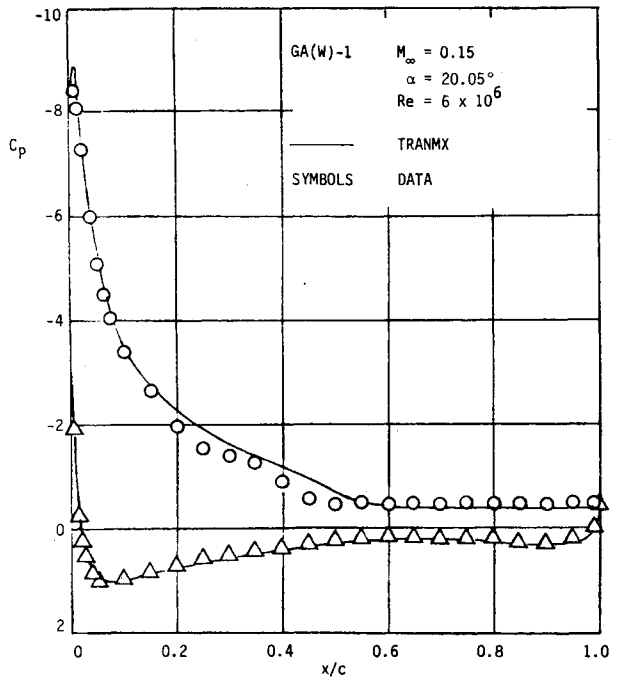

Fig. 6 Pressure distribution along GA(W)-1 airfoil.

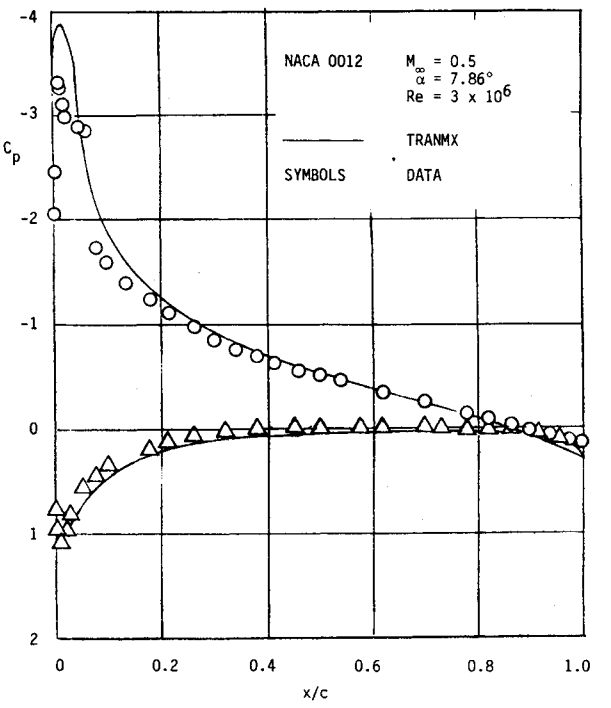

a) α = 7.86 deg.

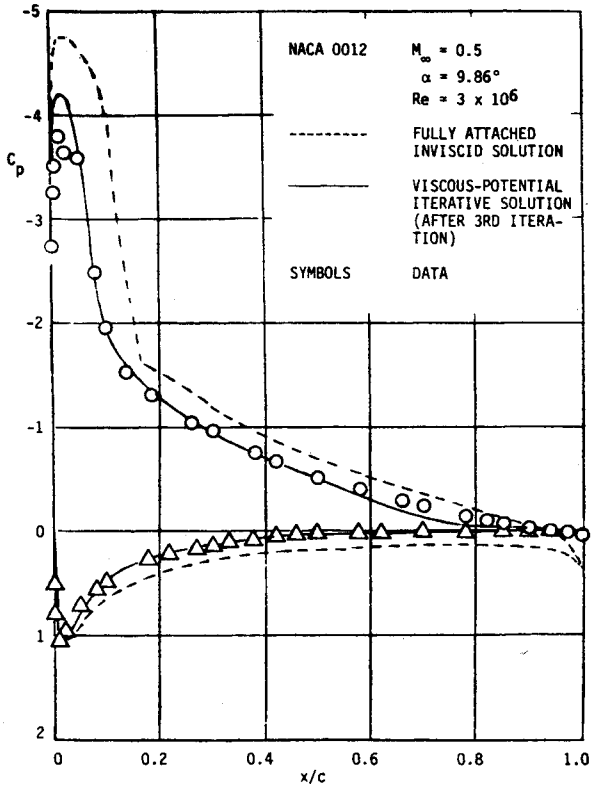

b) α = 9.86 deg.

Fig. 7 Pressure distribution along an NACA 0012 airfoil.

The case of the GA(W)-1 airfoil is of particular interest, since it can serve as an important yardstick for the performance of the present method. The freestream Mach number of 0.15 does not exhibit any complex phenomena of highly compressible transonic flow and, therefore, the performance of the calculation method can be attributed to the wake model used in the method. The present results (Fig. 6) are obtained for $M_\infty = 0.15$, $Re = 6 \times 10^6$ at $\alpha = 20.06$ deg (beyond the stall angle). The good correlation with the experiment confirms that the wake model provides physically realistic results.

The comparisons shown in Figs. 7 and 8 are for the NACA 0012 symmetric airfoil at $M_\infty = 0.5$, $Re = 3 \times 10^6$. Here again, the results are quite good, although the quoted angles of attack appear to be high. It is interesting to note that the pure inviscid solution for $\alpha = 9.86$ deg, which is plotted in Fig. 7b, fails to predict the real pressure distribution by a surprising margin. A separated region of about 20% of the chord makes the pure potential flow solution meaningless. This demonstrates that the viscid/inviscid iteration changes the real flowfield considerably, and the viscous effects cannot be ignored.

Results for a helicopter airfoil section (the A1 airfoil) are compared in Figs. 9-12. The data were collected by Hicks and McCroskey[15] in the Ames 2 × 2 ft Transonic Wind Tunnel. The $C_l - \alpha$ curve shown in Fig. 9 can be divided into three regions. The flow in the first region, $\alpha < 8$ deg, can be characterized by either fully attached flow or a small amount of trailing-edge separation. The lift C_l varies nearly linearly with respect to α in this region. The next region represents the flow for angles of attack from 8 deg to α_{CLMAX}. The boundary layer in this region separates at the foot of the shock and thus blunts the shock front. In this region, a combination of shock separation and trailing-edge separation is present. C_l continues to increase in this region until the point where catastrophic leading-edge separation brings it down sharply in the third region.

The results are in good agreement with experiment in Region I. The calculated C_l is much higher than the experimental data in Region II, although the general trend of the $C_l - \alpha$ curve is in close agreement with the experiment. The lower experimental C_l is due to the shock boundary-layer separation, which the present method currently cannot predict. The analysis predicts the break in the pitching moment distribution in Fig. 10. The pressure distributions shown in Figs. 11 and 12 correlate very well with the experimental data.

The new calculation method performs very well for all the cases tested. The minor discrepancies which exist in some of the comparisons are attributed to the calculation method's own limitations rather than inconsistent performance. Misleading high lift, which is likely to happen when the method does not detect the shock boundary-layer separation, can be easily noted by a careful analysis of the computed results. One obvious clue may be the unrealistically high local speed, say

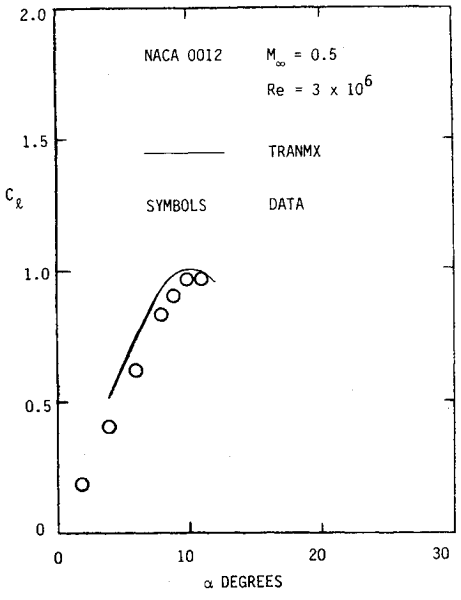

Fig. 8 $C_l - \alpha$ curve for NACA 0012 airfoil.

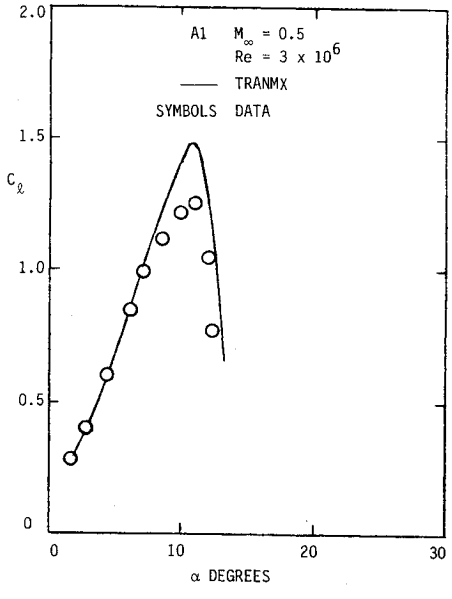

Fig. 9 $C_l - \alpha$ curve for A1 airfoil.

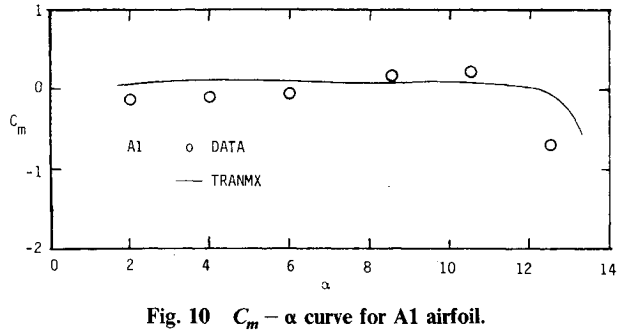

Fig. 10 $C_m - \alpha$ curve for A1 airfoil.

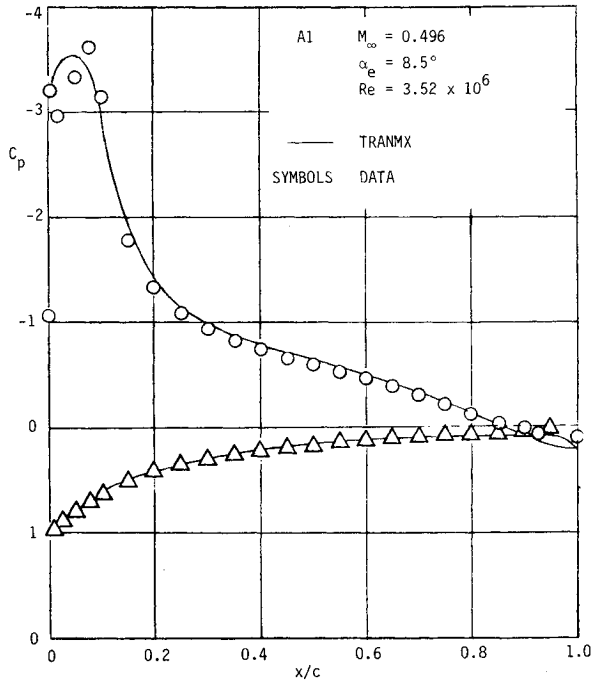

Fig. 11 Pressure distribution along an A1 airfoil for $M_\infty = 0.496$; $\alpha = 8.5$ deg.

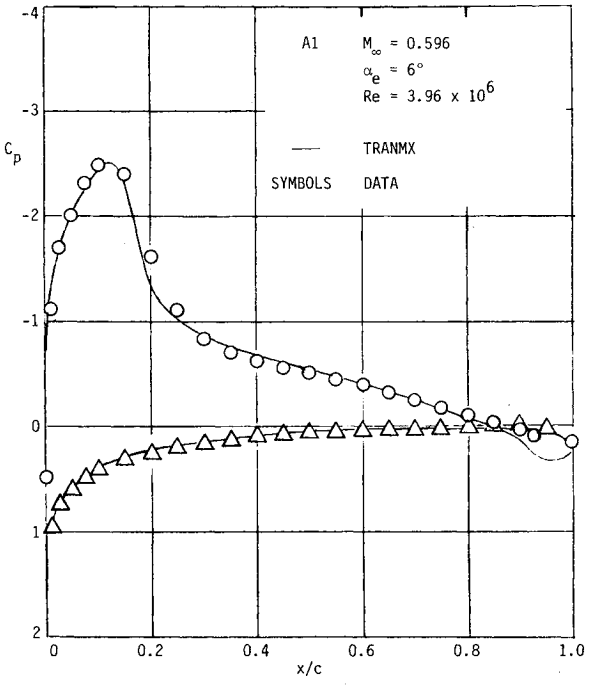

Fig. 12 Pressure distribution along an A1 airfoil for $M_\infty = 0.596$; $\alpha = 6$ deg.

$M > 1.4$, since the boundary layer through this shock is not likely to remain attached.

The main difficulty in verifying the calculation method has been the lack of quality transonic flow data. Most of the available data are limited to the case of no or small separated flow regions. In some cases, e.g., the A1 airfoil, the angle of attack correction due to tunnel wall interference is so large (for $M_\infty = 0.6$, $\Delta\alpha \approx 3$-5 deg) that comparisons with the data are difficult. More reliable high Mach number flow data with a substantial region of reversed flow are desired for the future improvement of the calculation method.

Conclusions

An analysis method for transonic trailing-edge-type separated flow has been demonstrated by comparison with experimental data. Predicted $C_l - \alpha$ behavior is in good agreement with experiment for several different airfoil types at Mach numbers approaching 0.6. At higher Mach numbers, inspection of the local Mach number distribution usually suggests separation as a result of strong shocks. While the program is not currently capable of modeling this phenomenon, it can be used as a predictive tool to indicate when shock/boundary-layer separation can be expected.

The main advantage of this method over other existing methods is that the present scheme with its simple wake model allows computations for massive separation. It also can be readily extended to the three-dimensional case.

Acknowledgments

This work was supported by the U.S. Army Research Office under Contract DAAG29-78-C-0004. The support of the Army Research Office and its Engineering Science Division Director, Dr. R.E. Singleton, is gratefully acknowledged.

References

[1]Hicks, R., private communication, NASA Ames Research Center, 1977.

[2]Diewert, G.S., "Computation of Separated Transonic Turbulent Flows," AIAA Paper 75-829, June 1975.

[3]Barnwell, R.W., "A Potential Flow/Boundary Layer Method for Calculating Subsonic and Transonic Airfoil Flow with Trailing-Edge Separation," NASA TM-81850, June 1981.

[4]Cousteix, J., *AFOSR-HTTM-Stanford Conference on Complex Turbulent Flows, Comparison of Computation and Experiment, Volume 1*, Stanford University, Stanford, Calif., 1981.

[5]Dvorak, F.A., Maskew, B., and Rao, B.M., "An Investigation of Separation Models for the Prediction of $C_{l_{max}}$," Final Technical Report, Contract DAAG29-76-C-0019, U.S. Army Research Office, Research Triangle Park, N.C., April 1979.

[6]Blascovich, J.D., "Characteristics of Separated Flow Airfoil Analysis Methods," Grumman Aerospace Corp., Bethpage, N.Y., Jan. 1983.

[7]Jameson, A., "Numerical Computation of Transonic Flows with Shock Waves," *International Union of Theoretical and Applied Mechanics*, Springer-Verlag, New York, 1975, pp. 384-414.

[8]Brune, G.W. and Manke, J.W., "An Improved Version of the NASA Lockheed Multielement Airfoil Analysis Computer Program," NASA CR-145323, March 1978.

[9]Green, J.E., Weeks, D.J., and Brooman, J.W.F., "Prediction of Turbulent Boundary Layers and Wakes in Compressible Flow by a Lag-Entrainment Method," Royal Aircraft Establishment TR-72231, Dec. 1972.

[10]Rogers, E.O., "Numerical Solution of Subcritical Flow Past Airfoils," NSRDC Rept. 4112, May 1973.

[11]Dvorak, F.A. and Woodward, F.A., "A Viscous/Potential Flow Interaction Analysis Method for Multi-Element Infinite Swept Wings," Vol. I, NASA CR-2476, Nov. 1974.

[12]Thwaites, B., "Approximate Calculation of the Laminar Boundary Layer," *Aeronautical Quarterly*, Vol. 1, Jan.-March, 1949, pp. 245-280.

[13]McGhee, R.J. and Beasley, W.D., "Low-Speed Aerodynamic Characteristics of a 17-Percent Thick Airfoil Section Designed for General Aviation Applications," NASA TN D-7428, Dec. 1973.

[14]NASA Langley Research Center, private communication, 1981.

[15]Hicks, R.M. and McCroskey, W.J., "An Experimental Evaluation of a Helicopter Rotor Section Designed by Numerical Optimization," NASA TM-78622, March 1980.